Journal of Biological Physics 31: 453–464, 2005.
DOI: 10.1007/s10867-005-6472-7

Red Blood Cell Shape and Fluctuations: Cytoskeleton Confinement and ATP Activity

N. GOV[1] and S.A. SAFRAN[2]
[1]*Department of Chemical Physics, Weizmann Institute of Science, Rehovot, Israel;* [2]*Department Materials and Interfaces, Weizmann Institute of Science, Rehovot, Israel*
(Authors for correspondence, [1]*e-mail: nir.gov@weizmann.ac.il,*
[2]*e-mail: sam.safran@weizmann.ac.il)*

Abstract. We review recent theoretical work that analyzes experimental measurements of the shape and fluctuations of red blood cells. Particular emphasis is placed on the role of the cytoskeleton and cell elasticity and we contrast the situation of elastic cells with that of fluid-filled vesicles. In red blood cells (RBCs), the cytoskeleton consists of a two-dimensional network of spectrin proteins. Our analysis of the wave vector and frequency dependence of the fluctuation spectrum of RBCs indicates that the spectrin network acts as a confining potential that reduces the fluctuations of the lipid bilayer membrane. However, since the cytoskeleton is only sparsely connected to the bilayer, one cannot regard the composite cytoskeleton membrane as a polymerized object with a shear modulus. The sensitivity of RBC fluctuations and shapes to ATP concentration may reflect the transient defects induced in the cytoskeleton network by ATP.

Key words: cytoskeleton, elasticity, membrane, fluctuations, erythrocytes, red blood cells

1. Introduction

Red blood cells must adapt to the relatively wide range of capillary sizes found in blood vessels; they must be at the same time deformable while maintaining their cellular integrity and function. This is possible because the cell shape is determined by the combination of a soft, fluid membrane (the lipid bilayer) and a two-dimensional, relatively rigid network (the spectrin cytoskeleton) that lies underneath the bilayer [1]. The coupling between the elastic cytoskeleton and the fluid, lipid membrane is important for understanding the mechanical properties and fluctuation spectrum of the cell [2, 3]. The details of the cytoskeleton components and their geometry vary between cells, but there are general features that are common to all: the fluid bilayer is attached to the cytoskeleton through specialized [4] membrane proteins, confined to small attachment patches of $\sim$10–50 nm each, that can be relatively sparse ($\sim$100 nm apart in the red blood cell (RBC) [5]). The cytoskeleton can either be a three dimensional actin gel that fills the entire cell volume or a thin, quasi-two dimensional, protein network as in RBC, and is usually much stiffer than the bilayer; its gel-like structure gives it a shear modulus. The fluctuations of that part of the bilayer that is attached to the cytoskeleton are therefore confined in the normal

and lateral directions. It is interesting to see how this highly inhomoge-neous confinement affects the entire membrane, including those sections that are not directly attached to the cytoskeleton.

RBCs have a two-dimensional cytoskeleton composed of an approximately hexagonal network of crosslinked, spectrin protein molecules. Measurements of the thermal fluctuations of the cell membrane result in [6, 7] amplitudes much larger than one would expect [8, 9] if one would attribute the full-shear modulus of the spectrin network to the bilayer membrane. Increasing the shear modulus of the spectrin network by the addition of additional crosslinking agents, has a negligible effect on the observed fluctuation amplitudes [9]. Recent models of RBC fluctuations [2, 3, 10] showed that the sparse nature of the coupling of the two-dimensional cytoskeleton of RBC to the membrane allows significantly larger membrane fluctuations than expected from a model in which the shear modulus of the cytoskeleton is also attributed to the bilayer membranes. The cytoskeleton does have some effect which results in an effective membrane tension [2, 3, 11] as well as a soft potential that confines the membrane fluctuations. Again, in contrast to "dead matter", the cytoskeletal elasticity is regulated by ATP that can change the nature of the actin-spectrin crosslinks. Defects in the cytoskeleton induced by ATP may explain the increase in fluctuations as the amount of ATP in RBCs is increased [10, 12]. Other cytoskeletal elastic effects that determine RBC shape include the formation of fold-lines [10, 13] in RBCs that are confined to narrow capillaries and to changes in the overall RBC shape [14–16] (echinocyte or discocyte formation). These effects are controlled by ATP, thus indicating how non-equilibrium processes are critical in determining even the steady-state shape of biological cells.

This brief review begins in the next section with a discussion of the elasticity of the two-dimensional spectrin network of red blood cells and its implications for the static and dynamic fluctuations of RBCs. The theoretical predictions are compared with experiments that determine the magnitude of the effective tension and confining potential induced by the cytoskeleton. The observed increase of the fluctuations with ATP activity and its release by deformed RBCs is discussed in terms of cytoskeletal defects induced by ATP.

2. Elasticity of Red Blood Cells

The shape of red blood cells is strongly determined by the mechanical properties of the cytoskeleton and by ATP activity. The surface of the RBC is a composite material containing an outer lipid bilayer, and an inner, two-dimensional cytoskeleton that is composed of the protein spectrin [5] attached in a sparse manner to the lipid bilayer [2, 3]. The links of the network consist of flexible spectrin molecules ($R \sim$ 80–100 nm), crosslinked at the network nodes by a complex containing a short ($\sim$30 nm) actin filament, band-4.1 and other proteins [4, 5]. We begin with a discussion of the cytoskeleton effects on the shape fluctuations of RBC and then consider the role of ATP in enhancing both the fluctuations as well as shape changes.

2.1. SHAPE FLUCTUATIONS

In this section, we focus on the effects of the inhomogeneous potential exerted by the spectrin network on the lipid bilayer and its effect on the thermal fluctuations [6] of the membrane. These fluctuations have been measured in RBC [7], and the effective membrane bending modulus κ was found to vary dramatically as a function of the measured wave vector q. These observations, as well as those of the temporal spectrum [12], have presented a theoretical challenge since they appear to indicate that the bilayer behaves as if it is almost detached from the underlying cytoskeleton [2, 8]. At the same time, the membrane acquires a wavelength-dependent surface tension, in addition to its curvature modulus [2, 3]. This tension is much larger than estimated from the finite size effect $\sigma \gg \kappa/R^2$ [6]. We have found that we can predict these properties using a simple, well-controlled model.

The simplest description of the membrane neglects the thickness of the cytoskeleton and the sparse attachments to the bilayer, and treats a bilayer that is completely attached to a two-dimensional (i.e. zero thickness) cytoskeleton [7, 8]. In this case, the membrane has, at all length scales, the bare bending modulus of the bilayer and the shear modulus of the cytoskeleton which is of the order of 6×10^{-6} J/m^2 [17]. This would be expected to show very small thermal fluctuations due to the large shear restoring force. However, this model is ruled out by the observed distribution of the fluctuation amplitude among different shape modes and over the RBC surface [7, 8]. We therefore must take into account the relatively weak coupling between the bilayer and cytoskeleton, due to the sparse connections and the soft nature of the cytoskeletal shell.

Our model accounts for the relatively large amplitude of RBC fluctuations, considering the relatively weak potential exerted on the membrane by the soft cytoskeletal shell sparsely attached to the bilayer. The average bilayer-shell distance is related to the observed amplitude of thermal fluctuations, and depends on the undulations of both the bilayer and spectrin filaments. The spectrin filaments form a connected, quasi-two-dimensional shell that has a three-dimensional thickness of $d \sim 30$ nm, due to the conformations of the soft filaments out of the plane of the shell. This can be modelled by a restoring force on the bilayer, which we account for via a harmonic potential. The force acts at all bilayer-spectrin distances due to the relatively delocalized and "soft" nature of the spectrin network. Additionally, the sparse attachment points of the membrane to this potential induce an effective surface tension in the bilayer [3]. The resulting free energy is therefore given by

$$F \simeq \int dS \left[\frac{1}{2}\sigma(\nabla h)^2 + \frac{1}{2}\kappa(\nabla^2 h)^2 + \frac{1}{2}\gamma h^2 \right] \tag{1}$$

where σ is the effective surface tension and γ describes the confining harmonic potential [2]. The spectrin filaments behave as entropic springs; they can have random conformations in the half-space beneath the lipid bilayer, since they are not strongly adsorbed to the bilayer, except at their ends [18]. This would predict a

fluctuation amplitude given by

$$\langle h_q^2 \rangle = \frac{k_B T}{\kappa_q q^4} \tag{2}$$

where κ_q is a renormalized bending modulus given by

$$\kappa/\kappa_q = \frac{\kappa}{\kappa + \sigma q^{-2} + \gamma q^{-4}} \tag{3}$$

where the bare bending modulus $\kappa \sim 2 \times 10^{-20}$ J.

We now analyze the static fluctuation spectrum, that is the height fluctuations as a function of the wave vector q [19]. In the limit of short wavelengths (large q) we find that the data for the mean-square amplitude is reasonably described by the expression for a free membrane: $\langle h_q^2 \rangle = k_B T/(\kappa q^4)$ with a bare bending modulus $\kappa \sim 2 \times 10^{-20}$ J. For the largest wave vectors the data are noisy due to experimental limitations. We view this value of κ as indicative of the bare value of the bilayer bending modulus, since, in this limit, the bilayer is largely free of the sparse cytoskeletal connections. The amplitude of fluctuations is also small compared with the average bilayer-cytoskeleton distance of $d \sim 30$ nm, so that interaction between the two is small.

In the other limit of small wave vectors, we find that the fluctuation amplitude saturates. In order to find the value of the parameters γ and σ we plot in Figure 1 the renormalized effective bending modulus κ_q (Eq. (3)). Using this plot we find the ratio γ/κ. Fitting the data, we get the following values for the small q range: $\gamma \sim 1$–8×10^7 J/m^4 and $\sigma \sim 5$–12×10^{-7} J/m^2, where the variability represents the natural spread of values among different cells. Using these values to fit the experimental data for the *absolute* amplitude of the static fluctuations, we find that it is enhanced by a factor of ∼3, which we attribute to an increased effective temperature $T_{\text{eff}}/T \sim 3$ due to the ATP-driven height fluctuations [10]. Note that exactly the same enhancement factor explains the measurements of the *dynamic* fluctuation amplitude in ATP-depleted and ATP-containing RBC ghosts (in very different experiments) showing the overall consistency of our description [3, 12].

For comparison, we consider the data for the stomatocyte cell [19]. These cells are known to have a weakened cytoskeleton and a much expanded bilayer [16]. The first effect is taken into account by a reduction of the surface tension σ and γ by ∼15%, since both are linearly dependent on the shear modulus of the cytoskeleton μ [3], which is reduced by this amount. The weaker cytoskeleton allows the bilayer to have a shape transition into a stomatocyte, that is characterized by a stretched bilayer [16]. In this case, ATP-induced defects in the cytoskeleton do not translate into normal motion of the bilayer, and the effective temperature is therefore found to be $T_{\text{eff}}/T \sim 1.2$.

The data for the echinocyte cell [19] fits with our expectation of increased surface tension and harmonic potential parameters by a factor of ∼2.2, compared

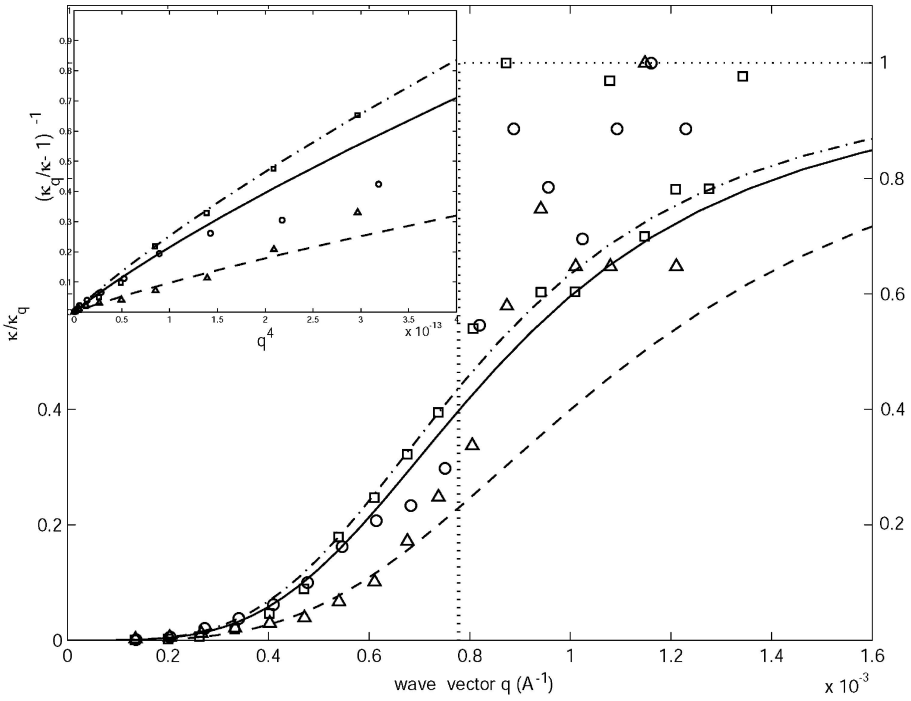

Figure 1. Calculated normalized effective bending modulus κ_q (Eq. (3)) compared with the experimental data [19]: normal cells – circles (solid line), stomatocyte – squares (dashed – dot line), echinocyte – triangles (dashed line). The vertical dotted line shows the crossover wavevector $q_0 \sim (\gamma/\kappa)^{1/4}$. The inset shows the same data in the limit of small q vectors, to determine the ratio γ/κ. The linearity in this plot at small values of q indicates that the value of γ (arising from the cytoskeletal potential) must be nonzero.

to the values for the normal RBC. We also expect the effective temperature to be essentially given by its bare, thermal value, since ATP activity is absent in the cytoskeleton of the echinocyte. Indeed, measurements of the effective absolute fluctuation amplitude are found to be ∼3.8 times smaller than for the normal RBC.

An extension of the static theory to treat the dynamical fluctuations has been presented in [2, 20, 21]; for the hydrodynamic analysis, the cytoskeleton can be taken to be a somewhat permeable wall that impedes water flow; this is in addition to its role as a source of membrane tension and a confining potential. We note that our analysis of the *dynamic* fluctuation data is consistent with an effective value of the average bilayer-cytoskeleton distance, $d \sim 30$ nm, which is determined by the soft potential strength, γ, deduced from our analysis of the *static* fluctuation data. The slow water flow, appropriate to the measurements of the low frequencies of dynamic bilayer fluctuations, is such that the cytoskeleton is nearly impermeable. This is because on the slow time scale of the water flow, the spectrin network fluctuates and effectively covers the entire two-dimensional plane. The transient, ATP-induced defects are much faster than these slow flows, so that the water is

bounded on one side by the bilayer and on the other side by the spectrin network [2] which, on average is at a distance d from the bilayer. Since the restoring force is constant, the ATP activity is best taken into account through an increased effective temperature, i.e. increased agitation force.

2.2. MICROSCOPIC MODEL

The phenomenological analysis presented above found that the sparse coupling of the cytoskeleton and the RBC membrane results in a description of a membrane characterized by three effective parameters: κ, σ, γ. In [3] we presented a microscopic model of a bilayer membrane in a periodic potential and showed that the phenomenological parameters, κ, σ, γ, have their origin in the long-wavelength limit of that microscopic model. The phenomenological parameters are shown to be related to the amplitude and wavelength of the potential that the cytoskeleton exerts on the membrane.

Our simplified microscopic model approximates the membrane cytoskeleton coupling as a periodic harmonic potential. The point of attachment of the cytoskeleton to the membrane is through relatively short and rigid protein complexes [1, 5] (e.g., p. 4.1, p. 55). The *flexible* spectrin filaments provide the smooth restoring force of the cytoskeleton that acts on the membrane and this motivates our harmonic approximation. The spectrin molecules behave as linear entropic springs, with non-linearity at large extensions [22], beyond the range of the thermal fluctuations discussed here. We studied two extreme situations for the lateral potential: a series of delta-functions, and a smooth sinusoidal function [3].

The Hamiltonian H of the membrane is written as

$$H = \int d\vec{r} \int d\vec{r}' \left[\frac{\kappa}{2} (\nabla^2 h)^2 + V(\vec{r} - \vec{r}') h(\vec{r}) h(\vec{r}') \right] \tag{4}$$

where κ is the bending modulus and $V(\vec{r} - \vec{r}')$ is the external potential that represents the inhomogeneous coupling to the cytoskeleton. For a localized, harmonic confining potential, the second term in (4) becomes $V(\vec{r})h(\vec{r})^2$. To calculate the correlations, we use a relation between the linear response of the membrane to a localized force, $f\delta(\vec{r})$, and the correlation function for membrane fluctuations [3, 6]. The real-space correlation function $\langle h(\vec{r})h(0)\rangle$ is related to the function $\chi(\vec{r})$ determined by the differential equation:

$$V(\vec{r})\chi(\vec{r}) + \kappa \nabla^4 \chi(\vec{r}) = f\delta(\vec{r}). \tag{5}$$

In [3] this equation is solved analytically for the case of a two-dimensional checkerboard potential characterized by a spatial variation proportional to $V_0 \cos(G_x)\cos(G_y)$ with the single wave vector $\vec{G}$. The approximation used neglects the coupling to higher harmonics and predicts an effective bending stiffness

$\bar{\kappa}$, effective tension $\bar{\sigma}$, and effective potential $\bar{\gamma}$ from an expansion of the height correlation function to fourth order in the wave vector. In the limit of both weak ($V_0/G^4\kappa \ll 1$) and strong ($V_0/G^4\kappa \gg 1$) confinement we have

$$\begin{aligned} &V_0 \to 0: \quad \bar{\gamma} \to V_0, \quad \bar{\sigma} \to -\frac{V_0^2}{8G^6\kappa}, \quad \bar{\kappa} \to \kappa \\ &V_0 \to \infty: \quad \bar{\gamma} \to \frac{3V_0}{4}, \quad \bar{\sigma} \to 2\kappa G^2, \quad \bar{\kappa} \to \frac{5}{4}\kappa. \end{aligned} \tag{6}$$

For weak confinement, both the curvature modulus and the confinement potential γ are easily understood; however we find a surprising, effective *negative* surface tension for weak potentials $V_0 < 4\kappa G^4$. In the limit of strong confinement, we find that the surface tension saturates to a positive value that is much larger than the tension due to finite size effects, with a somewhat renormalized bending modulus and monotonically increasing uniform confinement. The analytical approximation compares well with a numerical solution for long wavelength modulations (small values of $\vec{G}$) or small modulation amplitudes.

For both small and large values of $\vec{G}$ it is the "pulling" effect of the inhomogeneous pinning that induces the appearance of the effective surface tension. In the limit of $V_0 \to \infty$, the clamping has an effect that is similar to that of positive tension, σ, and the fluctuations are reduced. In the limit $V_0 \to 0$, there appears a wave vector q_0, at which the correlations are maximal; this is similar to the effect of buckling that a negative tension would induce.

Comparing the results of [3] with the fits to the static scattering experiments in RBC, we find in both cases that the predicted surface tension $\bar{\sigma} \sim 2 \times 10^{-7}\,\mathrm{J/m^2}$ is smaller than the measured value by a factor of ~3. The calculated surface tension is close to the asymptotic value of strong confinement $\bar{\sigma} \sim 2\kappa G^2$ (see Eq. (6)). Note also that the experimental value is about 30 times smaller than the cytoskeletal shear modulus ($\mu \sim 6 \times 10^{-6}\,\mathrm{J/m^2}$), while much larger than the surface tension arising from area conservation of the RBC: $\sigma_0 = \kappa/R^2 \sim 1 \times 10^{-9}\,\mathrm{J/m^2}$ (taking $R \sim 4\ \mu\mathrm{m}$ for the RBC radius) [2]. The surface tension imposed by the periodic potential is therefore distinct from both the cytoskeletal shear strength and the area conservation condition.

We now relate the values of the model parameters G and V_0 to the microscopic structure of the RBC cytoskeleton. The calculated periodicity is of the order of the observed average distance between cytoskeleton-bilayer connection sites (~150 nm) [7]. Additionally, the values of the peak confining harmonic potential exerted by the cytoskeleton, $V_0 \sim 100\ \kappa G^4$, can be related to the shear strength per unit area of the cytoskeleton μ: $V_0 \sim \mu G^2 \simeq 0.14\text{–}0.4 \times 10^8\ (\mathrm{J/m^4})$. The strength of the confinement that the cytoskeleton exerts on the lipid membrane at the coupling site, relates to cytoskeleton stiffness. This is because it is only the local shape changes of the cytoskeleton that provide a restoring force to the fluctuations of the lipid membrane, in addition to the intrinsic bending modulus of the bilayer.

This shows that both the effective potential, γ, as well as the tension, σ, have their origin in the periodicity, G, and shear modulus, μ, of the spectrin network.

Comparing the behavior of the model with the experiments as a function of wave vector, we find that the two-dimensional sinusoidal checkerboard potential can reproduce fairly well the low-q behavior, including the appearance of the relatively large effective surface tension. The measured data, though, shows a more abrupt change [11] around the crossover wave vector q_c (see Figure 4 of [3]).

Although the coupling of the cytoskeleton to the membrane occurs at distinct sites, the checkerboard model gives a surprisingly good approximation of the real cytoskeleton-bilayer coupling in the RBC, because of the diffusion induced fluctuations of these coupling points in the fluid, bilayer membrane. This is probably because the actual potential is smoothed by the fluctuations of the spectrin molecules and of the finite size patches that connect them to the membrane.

2.3. Activity and structure

In the absence of ATP, such as in depleted cells or washed ghosts, the r.m.s. amplitude at a given point in space of the bilayer thermal fluctuations (alone) is $\bar{h}_{\text{ther}} \sim 30\,\text{nm}$ [12]. When ATP is added, the fluctuation amplitude rises and saturates at physiological concentrations, giving $\bar{h} \sim 80\,\text{nm}$. In a previous discussion of the phenomenological model, we have shown that a consistent description of both the static and dynamic data is possible if we treat the ATP as introducing a higher effective temperature $T_{\text{eff}}/T \sim 3$ [2]. We now consider the origin of this effect.

The consumption of ATP is known to induce large membrane fluctuations [2, 12]. Since the hydrolysis of ATP releases $\Delta E_{\text{atp}} \sim 13 k_B T$, it provides more than enough energy to dissociate the spectrin from the actin at the nodes of the network; that energy cost is only $\Delta E_{\text{sa}} \sim 7 k_B T$. The rate of energy transfer by this mechanism into shape fluctuations of the membrane is limited by the following quantities: the elastic energy released in the membrane, the concentration of ATP, and the time it takes for the membrane to dissipate this energy and "reattach" to the cytoskeleton. The ATP-induced dissociations of spectrin are transient, because the dissociated spectrin can re-associate with the actin filament.

The adsorption of ATP to the phosphorylation sites at the spectrin-actin junctions can be described by the equilibrium occupation probability; this assumes that the ATP in the cytoplasm can be treated as a reservoir with concentration n_{ATP}. Standard thermodynamics gives

$$n_d = \frac{n_{\text{ATP}} e^{\varepsilon}}{1 + n_{\text{ATP}} e^{\varepsilon}} \tag{7}$$

where ε (in units of $k_B T$) is the energy to preferentially adsorb at the spectrin–actin sites as opposed to anywhere else on the membrane surface, and is given by the

following balance

$$\varepsilon \simeq \big(\Delta E_{\rm atp} - \Delta E_{\rm sa} - k_B S_f - \Delta E\big)/(k_B T)$$
$$\simeq 13 - 7 + 1.5 + 1.5 \simeq 9 \tag{8}$$

where S_f is the entropy change due to the release of the spectrin filament. The last term in Eq. (8) represents the mechanical energy released by the spectrin dissociation, estimated as $\Delta E \simeq \mu(R - R_0)^2 \simeq 1.5\, k_B T$, where μ is the cytoskeletal shear modulus, $R \sim 80$–100 nm is the typical spectrin network spacing, and $R_0 \sim 70$ nm is the ideal spectrin distance in the absence of the bilayer [10]. Due to the large adsorption energy, the ATP occupation of the spectrin–actin sites is saturated at relatively low ATP concentrations, in agreement with experimental data [12]. Dissociation of the actin–spectrin complex means that on both sides of the dissociated spectrin there are now transient, five-fold nodes that tend to buckle upwards [23] and can exert a force on the membrane. Thus, ATP-induced spectrin dissociation converts the stored elastic energy of the filament, into normal motion of the membrane. In addition, the dissociation can affect the membrane-cytoskeleton coupling proteins; this would also tend to increase the membrane fluctuations.

When the energy released by spectrin dissociation is added to the thermal energy $k_B T$ that is dissipated by each membrane mode, one predicts an enhanced effective temperature of the order of the measured factor of $T_{\rm eff}/T \sim 3$ [2]. Our estimate is valid under the condition that the ATP-induced processes, similar to the thermal motion of the membrane, are spatially incoherent. However, on the length-scale of the cytoskeleton network ($\sim$200 nm) itself, the motion is not thermal and does not satisfy the fluctuation-dissipation theorem [24]. The use of an effective temperature is only correct at larger scales where non-linear couplings mix the energy of the discrete motion into membranes modes of longer wavelength.

The local transfer of energy from the ATP to the membrane motion, on the scale of a single network element, can be estimated from the equation of motion for the local amplitude h of the membrane fluctuations (in the usual limit of large damping)

$$h(t) + \omega_{\rm m} h = \xi(t) \tag{9}$$

where a^2 is the area of the membrane contained in one network triangle (the mesh size of the spectrin network: $a \sim 80$ nm), η is the viscosity of the surrounding fluid and $\xi(t)$ is the normalized force, given by $\xi(t) = F(t)/(4a^2\eta k)$, where $k \sim 1/a$ and $F(t)$ is the actual force on the membrane that comes from the ATP included, transient disconnections of the spectrin chains from the network or of the spectrin-membrane coupling. For disconnections of the spectrin network, the force is derived from the energy ΔE discussed after Eq. (8). The first term on the left-hand side of Eq. (9)

represents the viscous damping of the membrane due to the surrounding fluid, and the second term is the restoring force due to the curvature stiffness of the bilayer. Here, $\eta \sim 3\eta_{\rm water}$ is a slightly enhanced, effective viscosity due to the cytoskeleton confinement of the membrane fluctuations [2, 20].

At the scale of a single spectrin network unit cell, the membrane has a characteristic fluctuation frequency: $\omega_{\rm m} \simeq \kappa/4\eta a^3 \sim 10^3\,{\rm Hz}$. This should also include the re-association time $\tau_{\rm re}$, which is the Zimm time it takes the detached end of the filament to thermally diffuse back to the attachment site, and reattach [25]. Since the detached spectrin is confined by the bilayer, only a short segment of the spectrin molecule can actually diffuse freely. This results in $\tau_{\rm re} \sim 10^{-7}$ sec, which can therefore be neglected.

For the RBC case, where $\omega_m \leq \tau^{-1}$ (in normal conditions), we can write

$$\langle |h|^2 \rangle_{\rm ATP} \simeq a^2 \frac{\Delta E}{\kappa} \frac{\mu a^2}{\kappa} \frac{n_d}{1 + (\tau\omega_{\rm m})^{-1}} \sim \frac{a^2}{6} n_d \tag{10}$$

where ΔE is the spectrin stretching energy defined above [10]. The maximal r.m.s. height fluctuation due to ATP is: $\langle |h|^2 \rangle_{\rm ATP}^{1/2} \sim a/\sqrt{6} \sim 40\,{\rm nm}$. Note that the ATP-induced amplitude is proportional to the ratio of the tension released in the cytoskeleton and the curvature modulus of the membrane. This means that the motion on the length-scale of the cytoskeleton network ($\sim$200 nm) is not thermal and does not satisfy the fluctuation-dissipation theorem [24, 26].

Our model for the effective temperature as a function of ATP concentration agrees rather well with the data, except at low ATP concentrations, where there seems to be a threshold behavior in the experiments [10]. This could arise from competing ATP-adsorption sites other than the spectrin-actin nodes that effectively lower the available ATP concentration.

In addition to enhancing the membrane fluctuations, ATP-induced transient defects of the spectrin network are also important in determining the average shape of RBCs [14, 15]. ATP is clearly important for maintaining the discocyte shape of a free RBC, since it has been observed that depletion of ATP causes a change from the discocyte to the echinocyte shape [16]. This change of shape suggests that the loss of ATP results in a stiffer cytoskeleton that pulls the bilayer over a smaller cytoskeletal projected area. The need to accommodate the bilayer area over a smaller projected area results in the appearance of the spicules of the echinocyte shape. In our model, the physical origin of this effect is simply related to the change in the number of released spectrin filaments, when the number of defects is reduced as ATP is reduced. We can estimate [10] this effect by estimating the resulting area difference between the interior and exterior membrane layers that has been suggested to drive the various shape transitions of RBC [16]. We relate this area difference to the pulling force that the cytoskeleton exerts on the bilayer, and predict its dependence on the ATP concentration.

Acknowledgments

The authors acknowledge very fruitful experimental collaborations with A. Bitler, R. Kornstein, E. Sackmann, H. Strey and theoretical collaborations with A. Zilman. This work has been supported by the Israel Science Foundation, the U.S.-Israel Binational Science Foundation and an EU Network Grant.

References

1. Alberts, B., Bray, D., Lewis, J., Raff, M., Roberts, K. and Watson, J.: *Molecular Biology of the Cell*, Garfand Publishing, New York, 1994.
2. Gov, N., Zilman, A. and Safran, S.: Cytoskeleton Confinement and Tension of Red Blood Cell Membranes, *Phys. Rev. Lett.* **90** (2003), 228101-1–228101-4.
3. Gov, N. and Safran, S.A.: Pinning of Fluid Membranes by Periodic Harmonic Potentials, *Phys. Rev. E* **69** (2004), 011101-1–011101-10.
4. Ling, E., Danilov, Y.N. and Cohen, C.M.: Modulation of Red Cell Band 4.1 Function by cAMP-Dependent Kinase and Protein Kinase C Phosphorylation, *J. Biol. Chem.* **263** (1988), 2209–2216.
5. Manno, S., Takakuwa, Y., Nagao, K. and Mohandas, N.: Modulation of Erythrocyte Membrane Mechanical Function ' by beta-Spectrin Phosphorylation and Dephosphorylation, *J. Biol. Chem.* **270** (1995), 5659–5665.
6. Bennett, V.: The Spectrin-Actin Junction of Erythrocyte Membrane Skeletons, *Bioch. Biophys. Acta* **988** (1989), 107–121.
7. Safran, S.A. (ed.): Statistical Thermodynamics of Surfaces, Interfaces, and Membranes, Westview Press, Boulder, CO, 2003.
8. Zilker, A., Engelhardt, H. and Sackmann, E.: Dynamic Reflection Interference Contract (RIC-) Microscopy: A New Method to Study Surface-Excitations of Cells, *J. de Physique* **48** (1987), 2139–2151.
9. Strey, H., Peterson, M. and Sackmann, E.: Measurement of Erythrocyte Membrane Elasticity by Flicker Eigenmode Decomposition, *Biophys. J.* **69** (1995), 478–488.
10. Peterson, M.A.: Linear Response of the Human Erthrocyte to Mechanical Stress, *Phys. Rev. A* **45** (1992), 4116–4135.
11. Peterson, M., Strey, H. and Sackmann, E.: Theoretical and Phase Contrast Microscopic Eigenmode Analysis of Erthrocyte Flicker Amplitudes, *J. Phys. H France* **2** (1992), 1273–1285.
12. Zeman, K., Engelhard, H. and Sackmann, E.: Bending Undulations and Elasticity of the Erthrocyte Membrane: Effects of Cell Shape and Membrane Organization, *Eur. Biophys. J.* **18** (1990), 203–219.
13. Gov, N. and Safran, S.A.: Red-Blood Cell Membrane Fluctuations and Shape Controlled by ATP-Induced Cytoskeletal Defects, *Biophys. J.* **88** (2005), 1859–1874.
14. Fournier, J.-B., Lacoste, D. and Raphael, E.: Fluctuation Spectrum of Fluid Membranes Coupled to an Elastic Meshwork: Jump of the Effective Surface Tension at The Mesh Size, *Phys. Rev. Lett.* **92** (2004), 018102-1–018102-4.
15. Tuvia, S., Levin, S., Bitler, A. and Korenstein, R.: Mechanical Fluctuations of the Membrane-Skeleton are Dependen ton F-Actin ATPase in Human Erythrocytes, *J. Cell Biol.* **141** (1998), 1551–1561.
16. Levin, S. and Korenstein, R.: Membrane Fluctuations in Erthrocytes are Linked to MgATP-Dependent Dynamic Assembly of the Membrane Skeleton, *Biophys. J.* **60** (1991), 733–737.
17. Evans, E.A.: Bending Elastic Modules of Red Blood Cell Membrane Derived from Buckling Instability in Micropipet Aspiration Tests, *Biophys. J.* **43** (1983), 27–30.

18. Dao, M., Lim, C.T. and Suresh, S.: Mechanics of the Human Red Blood Cell Deformed by Optical Tweezers, *J. Mech. Phys. Solids* **51** (2003), 2259–2280.
19. Hoffman, J.F.: Some Red Blood Cell Phenomenon for the Curious, *Blood Cells Mol. Dis.* **32** (2004), 335–340.
20. Hoffman, J.F.: Questions for Red Blood Cell Physiologists to Ponder in this Millenium, *Biol. Blood Cells Mol. Dis.* **27** (2001), 57–61.
21. Nakao, M.: New Insights into Regulation of Erythrocyte Shape, *Curr. Opin. Hem.* **9** (2002), 127–132.
22. Lim, H.W.G., Wortis, M. and Mukhopadhyay, R.: Stornocyte-Discocyte-Echinocyte Sequence of the Human Red Blood Cell: Evidence for the Bilayer-Couple Hypothesis from Membrane Mechanics. *P-Natl. Acad. Sci. U.S.A.* **99** (2002), 16766–16769.
23. Discher, D., Mohandas, N. and Evans, E.A.: Molecular Maps of Red Cell Deformation: Hidden Elasticity and *in situ* connectivity, *Science* **266** (1994), 1032–1035.
24. Engelhardt, H., Gaub, H. and Sackmann, E.: Viscoelastic Properties of Erythrocyte-Membranes in High-Frequency Electric-Fields, *Nature* **307** (1984), 378–380.
25. Everaers, R., Graham. I.S., Zuckermann, M.J. and Sackmann, E.: Entropic Elasticity of End Absorbed Polymer Chains: The Spectrin Network of Red Blood Cells as C*-Gel, *J. Chem. Phys.* **104** (1996), 3774–3781.
26. Zilker, A., Engelhardt. H. and Sackmann, E.: Dynamic Reflection Interference Contrast (RIC-) Microscopy – A New Method to Study Surface Excitations of Cells and to Measure Membrane Bending Elastic-Moduli, *J. de Physique* **48** (1987), 2139–2151.
27. Gov, N., Zilman, A. and Safran, S.A.: Hydrodynamic of Confined Membranes, *Phys. Rev. E* **70** (2004), 0111041–01110410.
28. Brochard, F. and Lennon, J.F.: Frequency Spectrum of the Flicker Phenomenon in Erthrocytes, *J. de Physique* **36** (1975), 1035–1047.
29. Discher, D.E. and Carl, P.: New Insights into Red Cell Network Structure, Elasticity, and Spectrin Unfolding – A Current Review, *Cell Mol. Biol. Lett.* **6** (2001), 593–606.
30. Seung, H.S. and Nelson, D.R.: Defects in Flexible Membranes with Crystalline Order, *Phys. Rev. A* **38** (1988), 1005–1018.
31. Carraro, C. and Nelson. D.R.: Grain-Boundary Buckling and Spin-Glass Models of Disorder in Membranes, *Phys. Rev. E* **48** (1993), 3082–3090.
32. Lidmar, J., Mirny, L. and Nelson, D.R: Virus Shapes and Buckling Transitions in Spherical Shells, *Phys. Rev. E* **68** (2003), 0519010-1–051910-10.
33. Liverpool, T.B.: Anomalous Fluctuations of Active Polar Filaments, *Phys. Rev. E* **67** (2003), 031909-1–031909-5.
34. Doi, M.: *Introduction to Polymer Physics*, Clarendon Press, Oxford, 1996.
35. Hitler, A. and Korenstein, R.: (submitted).